PERGAMON

International Journal of Solids and Structures 40 (2003) 5511–5519

INTERNATIONAL JOURNAL OF SOLIDS and STRUCTURES

www.elsevier.com/locate/ijsolstr

Theoretical model of piezoelectric fibre pull-out

Hong-Yuan Liu [a,*], Qing-Hua Qin [a], Yiu-Wing Mai [a,b]

[a] *Centre for Advanced Materials Technology (CAMT), School of Aerospace, Mechanical and Mechatronic Engineering J07, The University of Sydney, Sydney, NSW 2006, Australia*

[b] *MEEM, City University of Hong Kong, 83 Tat Chee Avenue, Kowloon, Hong Kong*

Received 30 October 2001; received in revised form 2 April 2003

Abstract

A theoretical model of a single piezoelectric fibre pull-out is developed to study the interaction between fibre deformation, pull-out stress and corresponding electrical field. Computer simulation of the stress–displacement curve of the fibre pull-out process is presented. Numerical examples show that the piezoelectric fibre pull-out behaviour can be both described and affected by its electrical field. Therefore, the interactions between the mechanical and electric fields of the fibre/matrix system can be employed to monitor and control the fracture behaviour of active fibre composites.
© 2003 Elsevier Ltd. All rights reserved.

Keywords: Piezoelectric fibre; Fibre pull-out; Active fibre composite

1. Introduction

Fracture in composites, whether crack growth transverse to fibres or interlaminar delamination, is a major concern in many applications, especially in aerospace where high structural reliability is required. Among various mechanisms contributing to the fracture resistance of composite materials, bridging by reinforcing fibres is considered to be one of highest interest because it provides direct closure traction to the bridged crack. In the past decade, several models have been proposed to investigate the relationship between crack growth and fibre bridging stress and efforts have been focused to enhance the fracture resistance of composites by providing sufficient bridging stresses on the crack faces (Xia et al., 1993; Cox, 1993; Cox and Marshall, 1994; Xia et al., 1994; Zok et al., 1997; Buchanan et al., 1997). In mode I crack growth, the bridging fibre experiences elastic deformation, debonding from the surround matrix and, finally, frictional pull-out. This process is collectively called "fibre pull-out", which can be described by a curve of bridging stress versus crack-opening displacement. Since the pull-out process is highly dependent on the bonding strength of the fibre and matrix (Kim and Mai, 1998), the traditional ways to enhance the bridging stress are to modify the interface adhesion between the fibre and matrix (Kim and Mai, 1998; Zhang et al., submitted for publication; Evans and Dalgleish, 1993; Budiansky et al., 1995; Bennett and Young, 1998;

* Corresponding author. Tel.: +61-2-9351-7148; fax: +61-2-9351-3760.
E-mail address: liu_hy@mech.eng.usyd.edu.au (H.-Y. Liu).

0020-7683/$ - see front matter © 2003 Elsevier Ltd. All rights reserved.
doi:10.1016/S0020-7683(03)00277-4

Larson and Miles, 1998; Kim and Mai, 1991). However, there are still some uncertainties with this technique. Firstly, the interface parameters are difficult to monitor during the manufacturing process. Currently, fibre surface treatment and sizing are used to enhance the interface bond strength. But the extent of the enhancement is rather hard to quantify. Secondly, with the rapid expansion of fibre composite applications, both high strength and high toughness are required in complex working conditions in which extreme temperature change, dynamic loads and impacts are experienced. Hence, traditional fibre composites, even with proper interface bonding, may not be able to provide stable performance under these environments. A "smart" fibre composite material, which has a high reliability against failure, is needed to meet these demanding challenges.

In recent years, a new "smart" fibre composite: active fibre composite that is made up of reinforcing fibres, piezoelectric fibres and resin matrix has been developed. It is an innovative combination of active fibres, passive fibres and matrix to create a new hybrid material for increasing high demands of current and upcoming applications (Bent, 1997). A piezoelectric fibre produces an electric field when it deforms. Vice versa, it undergoes deformation when subjected to an electric field. This function leads to a new conception that the mechanical behaviour can be both detected and controlled by the electric fields in the piezoelectric fibres.

This paper presents a theoretical model of the fibre pull-out for the simulation of the relationship between crack-opening and bridging stress. A solution of the interaction between the stress and electric field has been obtained. Numerical examples from this work show that, during the active fibre pull-out, an increment of the fibre deformation produces an increment of the pull-out stress which, in turn, causes a change of the electric field in the piezoelectric fibre. Therefore, the amount of fibre displacement can be detected by measuring the electric output. Conversely, changing the electric field also changes the pull-out stress which, consequently, affects the fibre displacement. This study is expected to provide a theoretical base towards an active control on the bridging stress of active fibre composites.

2. Stress field

A mechanics model of a single fibre pull-out test is shown in Fig. 1. A piezoelectric fibre with a radius a is embedded in a coaxial cylindrical matrix with an outer radius R. An initial debonded region of length l is present at the loaded fibre end. The length of the fibre is L. The matrix is considered as transversely isotropic (Timoshenko and Goodier, 1970), i.e.

$$\begin{pmatrix} \varepsilon^r \\ \varepsilon^\theta \\ \varepsilon^z \\ \gamma^{rz} \end{pmatrix} = \begin{pmatrix} s_{11} & s_{12} & s_{13} & 0 \\ s_{12} & s_{11} & s_{13} & 0 \\ s_{13} & s_{13} & s_{33} & 0 \\ 0 & 0 & 0 & s_{55} \end{pmatrix} \begin{pmatrix} \sigma^r \\ \sigma^\theta \\ \sigma^z \\ \tau^{rz} \end{pmatrix} + \begin{pmatrix} \varepsilon^{tt} \\ \varepsilon^{tt} \\ \varepsilon^t \\ 0 \end{pmatrix} \tag{1}$$

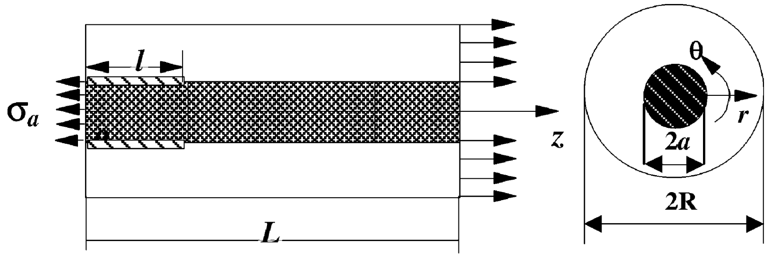

Fig. 1. Mechanics model of a fibre pull-out specimen with a partially debonded interface.

where, ε^t and ε^{tt} are axial and radial residual strains risen from curing process. s_{ij} are components of elastic compliance, ε^i, γ^{rz} and σ^i, τ^{rz} $(i = r, \theta, z)$ are strain and stress components, respectively.

The fibre is transversely isotropic and piezoelectric, i.e. (Qin, 2001),

$$\begin{pmatrix} \varepsilon^r \\ \varepsilon^\theta \\ \varepsilon^z \\ \gamma^{rz} \end{pmatrix} = \begin{bmatrix} s'_{11} & s'_{12} & s'_{13} & 0 \\ s'_{12} & s'_{11} & s'_{13} & 0 \\ s'_{13} & s'_{13} & s'_{33} & 0 \\ 0 & 0 & 0 & s'_{55} \end{bmatrix} \begin{pmatrix} \sigma^r \\ \sigma^\theta \\ \sigma^z \\ \tau^{rz} \end{pmatrix} + \begin{bmatrix} 0 & g_{31} \\ 0 & g_{31} \\ 0 & g_{33} \\ g_{15} & 0 \end{bmatrix} \begin{pmatrix} D^r \\ D^z \end{pmatrix} + \begin{pmatrix} \varepsilon^{tt} \\ \varepsilon^{tt} \\ \varepsilon^t \\ 0 \end{pmatrix} \tag{2}$$

and

$$\begin{pmatrix} E^r \\ E^z \end{pmatrix} = -\begin{bmatrix} 0 & 0 & 0 & g_{15} \\ g_{31} & g_{31} & g_{33} & 0 \end{bmatrix} \begin{pmatrix} \sigma^r \\ \sigma^\theta \\ \sigma^z \\ \tau^{rz} \end{pmatrix} + \begin{bmatrix} e_{11} & 0 \\ 0 & e_{33} \end{bmatrix}^{-1} \begin{pmatrix} D^r \\ D^z \end{pmatrix} \tag{3}$$

in which, D_i and E_i are components of the electric displacement ($\mathrm{N\,V^{-1}\,m^{-1}}$) and electric field ($\mathrm{V\,m^{-1}}$); g_{ij} and e_{ii} are piezoelectric coefficient ($\mathrm{V\,m\,N^{-1}}$) and dielectric constant ($\mathrm{N\,V^{-2}}$) (Qin, 2001).

The equilibria between the matrix axial stress, fibre axial stress and interfacial shear stress are given by

$$\frac{d\sigma_m^z}{dz} = \frac{2\gamma}{a}\tau_a \tag{4}$$

$$\frac{d\sigma_f^z}{dz} = -\frac{2}{a}\tau_a \tag{5}$$

where, subscripts 'f', 'm' and 'a' denote fibre, matrix and interface and $\gamma = a^2/(R^2 - a^2)$. The outer boundary conditions of the matrix are given by

$$\sigma_m^r\big|_{r=R} = 0, \qquad \tau_m^{rz}\big|_{r=R} = 0 \tag{6}$$

At the interface, the radial stresses and displacements of the fibre and matrix satisfy

$$\sigma_m^r\big|_{r=a} = \sigma_f^r\big|_{r=a} = q_i, \qquad u_m^r\big|_{r=a} = u_f^r\big|_{r=a} \tag{7}$$

where, q_i is the interfacial radial stress including thermal residual stress and Poisson contraction.

At the debonded interface, $0 \leqslant z \leqslant l$, the interfacial shear stress is determined by the Coulomb's friction law, that is

$$\tau_a = -\mu q_i \tag{8}$$

in which, μ is the friction coefficient.

At the bonded interface, $l \leqslant z \leqslant L$, the continuity of axial deformations require that

$$u_m^z\big|_{r=a} = u_f^z\big|_{r=a} \tag{9}$$

By Gauss' law, the electric displacements satisfy (Qin, 2001)

$$\frac{\partial D^r}{\partial r} + \frac{D^r}{r} + \frac{\partial D^z}{\partial z} = 0 \tag{10}$$

The relationship between the electric field, E, and the electric potential, Φ, is given by

$$E^r = -\frac{\partial \Phi}{\partial r}, \qquad E^z = -\frac{\partial \Phi}{\partial z} \tag{11}$$

Based on the results of our previous study (Zhang et al., 1999), all normal strains in the fibre are approximately independent of the radial coordinate, r. To simplify the calculations, here we assume that the electric potential, which is caused by the deformation of the fibre is also independent of the radial coordinate, i.e.,

$$\Phi = \Phi(z) \tag{12}$$

Using Eqs. (3) and (10)–(12), the relationship between the electric displacement and fibre axial stress for the piezoelectric fibre without an electric input is obtained as

$$D_z = d_{15}\sigma_f^z \tag{13}$$

where, d_{15} is a piezoelectric coefficient and given by $d_{ij} = g_{ij} \times e_{33}$.

Combining Eqs. (1)–(13) with the basic equations of elasticity (Timoshenko and Goodier, 1970) and following the same procedure and assumptions as in our early work (Zhang et al., 1999; Liu et al., 1999), the differential equations of the fibre axial stress, σ_f^z, are obtained as

$$\frac{d^2\sigma_f^z}{dz^2} - \frac{aC_3}{2\mu}\frac{d\sigma_f^z}{dz} - (C_1 + C_5 g_{31} d_{15})\sigma_f^z = C_2\sigma_a + C_4\sigma^T \quad (0 \leqslant z \leqslant l) \tag{14}$$

$$\begin{cases} \dfrac{d^2\sigma_f^z}{dz^2} - (C_1 + C_5 g_{31} d_{15})\sigma_f^z = C_2\sigma_a + C_3 q_i + C_4\sigma^T \\ \dfrac{d^2\sigma_f^z}{dz^2} - (F_1 + F_5 g_{33} d_{15})\sigma_f^z = F_2\sigma_a + F_3 q_i + F_4\sigma^T \end{cases} \quad (l \leqslant z \leqslant L) \tag{15}$$

All parameters C_i and F_i in Eqs. (14) and (15) are given in Appendix A.

Solving Eqs. (14) and (15) with boundary conditions at the ends of two intervals:

$$\sigma_f^z(0) = \sigma_a, \quad \sigma_f^z(L) = 0, \quad \sigma_f^z(l)^+ = \sigma_f^z(l)^- = \sigma_d \tag{16}$$

the solutions of the axial stress in the piezoelectric fibre are given by

$$\sigma_f^z(z) = k_1^d e^{\lambda_1 z} + k_2^d e^{\lambda_2 z} - k_3^d\sigma_a - k_4^d\sigma^T \quad (0 \leqslant z \leqslant l) \tag{17}$$

and

$$\sigma_f^z(z) = k_1^b \sinh\lambda z + k_2^b \cosh\lambda z - k_3^b\sigma_a - k_4^b\sigma^T \quad (l \leqslant z \leqslant L) \tag{18}$$

where the parameters k_i^b and k_i^d are also given in Appendix A.

With debonding and friction criteria (Zhang et al., 1999)

$$\tau_a(l)^+ = \tau_s, \qquad \tau_a(0)^+ = 0 \tag{19}$$

the applied stress, σ_a, and the debond tip stress, σ_d, can be obtained for a given debonding length.

3. Fibre displacement

From Eqs. (2) and (13), the fibre axial strain is given by (Liu et al., 1999)

$$\varepsilon_f^z = 2s'_{13}q_i + (s'_{33} + g_{33}d_{15})\sigma_f^z \tag{20}$$

By integrating Eq. (20) with the boundary conditions

$$u_f^z(L) = 0, \qquad u_f^z(l)^+ = u_f^z(l)^- = u^l \tag{21}$$

The displacement at the fibre end, δ, can be solved, i.e.,

$$\begin{aligned}\delta &= -u_{\mathrm{f}}^z(0)\\ &= k_1^{\mathrm{d}}\left(\frac{as'_{13}}{\mu}+\frac{s'_{33}+g_{33}d_{15}}{\lambda_1}\right)(\mathrm{e}^{\lambda_1 l}-1)+k_2^{\mathrm{d}}\left(\frac{as'_{13}}{\mu}+\frac{s'_{33}+g_{33}d_{15}}{\lambda_2}\right)(\mathrm{e}^{\lambda_2 l}-1)\\ &\quad -(s'_{33}+g_{33}d_{15})(k_3^{\mathrm{d}}\sigma_{\mathrm{a}}+k_4^{\mathrm{d}}\sigma^T)l-u^l\end{aligned} \tag{22}$$

where

$$u^l=\frac{w_1}{\lambda}[k_1^{\mathrm{b}}(\cosh\lambda l-\cosh\lambda L)+k_2^{\mathrm{b}}(\sinh\lambda l-\sinh\lambda L)]+(w_2\sigma_{\mathrm{a}}+w_4\sigma^T)(l-L) \tag{23}$$

and

$$w_1=s'_{33}+g_{33}d_{15}+\frac{2s'_{13}}{F_3-C_3}[C_1-F_1+d_{15}(C_5g_{31}-F_5g_{33})] \tag{24}$$

$$w_2=2s'_{13}\frac{C_2-F_2}{F_3-C_3}-w_1k_3^{\mathrm{b}} \tag{25}$$

$$w_4\sigma^T=2s'_{13}\frac{C_4\sigma^T-F_4\sigma^T}{F_3-C_3}-w_1k_4^{\mathrm{b}}\sigma^T \tag{26}$$

4. Electrical output

From Eq. (3), the electric field component E_z is given as

$$E_z=-\frac{1}{e_{33}}[(d_{33}-d_{15})\sigma_{\mathrm{f}}^z+2d_{31}q_i] \tag{27}$$

Using the solution of the stress field obtained in Section 2, the electric field can be calculated for both bonded and debonded regions. The difference of the electric potential at the two ends, $z=0$ and $z=L$, can be obtained by integrating

$$\Delta\Phi=-\int_0^L E_z\,\mathrm{d}z. \tag{28}$$

5. Numerical examples

Numerical examples are given for a piezoceramic/epoxy system, of which, the material parameters are (Liu et al., 1999; Piezo System, Inc., 1999): $s_{11}=s_{33}=0.33$ (GPa)$^{-1}$, $s_{12}=s_{13}=-0.13$ (GPa)$^{-1}$, $s_{55}=0.93$ (GPa)$^{-1}$, $s'_{11}=0.019$ (GPa)$^{-1}$, $s'_{33}=0.015$ (GPa)$^{-1}$, $s'_{12}=-0.0057$ (GPa)$^{-1}$, $s'_{13}=-0.0045$ (GPa)$^{-1}$, $s'_{55}=0.039$ (GPa)$^{-1}$. The radii of the matrix and fibre are 3 and 0.065 mm, respectively. The piezoelectric parameters of the fibre are given by (Piezo System, Inc., 1999; Pizzochero, 1998): $d_{33}=390\times10^{-12}$ m V^{-1}, $d_{31}=-d_{15}=-190\times10^{-12}$ m V^{-1}, $g_{33}=24\times10^{-3}$ V m N^{-1}, $g_{31}=-11.6\times10^{-3}$ V m N^{-1}, $e_{33}=16.25\times10^{-9}$ N V^{-2}. The residual strains of the fibre and matrix are: $\varepsilon_{\mathrm{f}}^t=\varepsilon_{\mathrm{f}}^{tt}=-4\times10^{-4}$ (Piezo System, Inc., 1999) and $\varepsilon_{\mathrm{m}}^t=\varepsilon_{\mathrm{m}}^{tt}=-65\times10^{-4}$ (Liu and Mai, 2000). The interfacial properties are approximately evaluated as $\tau_{\mathrm{s}}=0.04$ GPa and $\mu=0.8$ (Pizzochero, 1998; Liu and Mai, 2000).

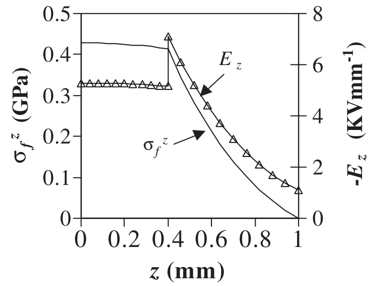

Fig. 2. Stress and electric fields in the piezoelectric fibre.

Fig. 2 shows the stress and electric fields in the piezoelectric fibre, where the debonding length is 0.4 mm. In the debonded region ($0 \leqslant z \leqslant 0.4$), both the fibre axial stress and electric field are nearly constant. In the bonded area, their values reduce rapidly. In the boundary between the bonded and debonded regions, E_z has a significant increment. This discontinuous behaviour is very similar to the discontinuous increment of the interfacial shear stress at that point (Zhang et al., 1999).

A computer simulation of a fibre pull-out stress–displacement curve is given in Fig. 3. With increasing displacement, the fibre stress increases until unstable debonding occurs. The variation of the electric output, $\Delta\Phi$, with displacement shows that the whole process can be detected electrically.

The interaction between the stress and electric fields is shown in Fig. 4. The stress–displacement curves are obtained by three different electric displacements. In this example, the electric displacement is controlled

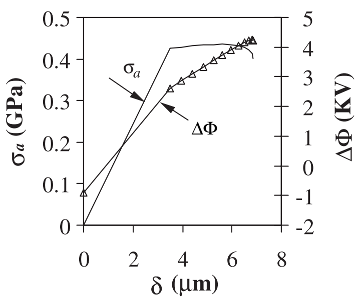

Fig. 3. Computer simulation of the bridging stress–fibre end displacement curve with corresponding electric output.

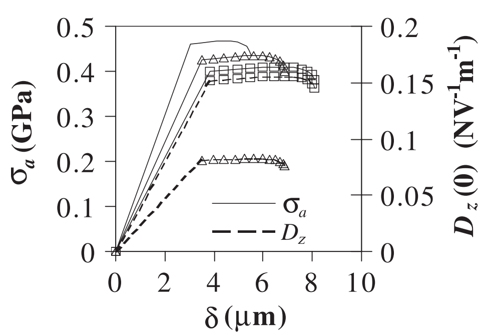

Fig. 4. Effect of electric displacement on stress–displacement curve, where (—) $d_{15} = 0$, (Δ) d_{15} and ($\square$) $2d_{15}$.

by its piezoelectric strain coefficient, d_{15}. It is clear that different electric displacements can make significant changes in the stress–displacement curves. Therefore, the relationship between the bridging stress and the crack-opening can be affected by the electric displacement. In this example, the change of the electric displacement is caused by its piezoelectric strain coefficient, d_{15}. In our further work, the stress–displacement curve as changed by the electric input will be discussed. Since the fracture resistance of a fibre composite is highly dependent on the stress–displacement curve of the fibre, it is expected that the fracture behaviour can be controlled electrically.

6. Conclusion

A theoretical model of a single piezoelectric fibre pull-out has been presented. Using this model, the relationship between the fibre bridging stress and crack-opening is obtained by computer simulation. The stress and electric fields are illustrated for a piezoceramic/epoxy system. The numerical examples show that the stress field and the electric field have a significant effect on each other. It can be concluded that piezoelectric fibres can be used to monitor the fracture behaviour of fibre composites.

Acknowledgements

The authors would like to thank the Australian Research Council (ARC) for the continuing support of this project by an ARC Large Research Grant awarded to H.-Y. Liu and Y.-W. Mai. H.-Y. Liu, Q.-H. Qin and Y.-W. Mai are supported by a Research Fellowship, a Professorial Fellowship and a Federation Fellowship, respectively, all by ARC.

Appendix A

$$C_1 = C_5(\gamma s_{13} + s'_{13}) \tag{A.1}$$

$$C_2 = -C_5\gamma s_{13} \tag{A.2}$$

$$C_3 = C_5[(1+\gamma)s_{11} - s_{12} + s'_{11} + s'_{12}] \tag{A.3}$$

$$C_4\sigma^T = C_5(\varepsilon_{\mathrm{f}}^{tt} - \varepsilon_{\mathrm{m}}^{tt}) \tag{A.4}$$

$$C_5 = -\frac{2}{as_{11}\overline{C}} \tag{A.5}$$

$$\overline{C} = F_1(a) - (1+2\gamma)F(a) + 2(1+\gamma)F(R) \tag{A.6}$$

$$F_1 = F_5(\gamma s_{33} + s'_{33}) \tag{A.7}$$

$$F_2 = -F_5 s_{33}\gamma \tag{A.8}$$

$$F_3 = 2F_5(\gamma s_{13} + s'_{13}) \tag{A.9}$$

$$F_4\sigma^T = F_5(\varepsilon_\mathrm{f}^t - \varepsilon_\mathrm{m}^t) \tag{A.10}$$

$$F_5 = -\frac{2}{as_{13}\overline{C}} \tag{A.11}$$

$$F(a) = \frac{\gamma}{a}\left\{\frac{R^2}{2} - \frac{a^2}{4} + \frac{s_{55}}{s_{13}}\left[\frac{a^2}{8} - \frac{R^2}{2}\left(\ln a - \frac{1}{2}\right)\right]\right\} \tag{A.12}$$

$$F(R) = \frac{\gamma R^2}{8a}\left\{2 + \frac{s_{55}}{s_{13}}\left[1 - 4\left(\ln R - \frac{1}{2}\right)\right]\right\} \tag{A.13}$$

$$F_1(a) = \frac{\gamma}{a}\frac{s_{55}}{s_{13}}\left(R^2 \ln a - \frac{a^2}{2}\right) + F(a) \tag{A.14}$$

$$\lambda = \sqrt{\frac{C_1F_3 - C_3F_1 - \overline{F}}{F_3 - C_3}} \tag{A.15}$$

$$\overline{F} = d_{15}(F_5C_3g_{33} - F_3C_5g_{31}) \tag{A.16}$$

$$\lambda_{1,2} = \frac{\frac{aC_3}{2\mu} \pm \sqrt{\left(\frac{aC_3}{2\mu}\right)^2 + 4(C_1 + C_5g_{31}d_{15})}}{2} \tag{A.17}$$

$$k_1^\mathrm{d} = \frac{1}{\mathrm{e}^{\lambda_2 l} - \mathrm{e}^{\lambda_1 l}}\left\{\sigma_\mathrm{a}[\mathrm{e}^{\lambda_2 l} + k_3^\mathrm{d}(\mathrm{e}^{\lambda_2 l} - 1)] - \sigma_\mathrm{d} + k_4^\mathrm{d}\sigma^T(\mathrm{e}^{\lambda_2 l} - 1)\right\} \tag{A.18}$$

$$k_2^\mathrm{d} = -\frac{1}{\mathrm{e}^{\lambda_2 l} - \mathrm{e}^{\lambda_1 l}}\left\{\sigma_\mathrm{a}[\mathrm{e}^{\lambda_1 l} + k_3^\mathrm{d}(\mathrm{e}^{\lambda_1 l} - 1)] - \sigma_\mathrm{d} + k_4^\mathrm{d}\sigma^T(\mathrm{e}^{\lambda_1 l} - 1)\right\} \tag{A.19}$$

$$k_3^\mathrm{d} = \frac{C_2}{C_1 + d_{15}C_5g_{31}} \tag{A.20}$$

$$k_4^\mathrm{d}\sigma^T = \frac{C_4\sigma^T}{C_1 + d_{15}C_5g_{31}} \tag{A.21}$$

$$k_1^\mathrm{b} = \frac{-1}{\sinh\lambda(L-l)}[k_3^\mathrm{b}\sigma_\mathrm{a}(\cosh\lambda L - \cosh\lambda l) + \sigma_\mathrm{d}\cosh\lambda L + k_4^\mathrm{b}\sigma^T(\cosh\lambda L - \cosh\lambda l)] \tag{A.22}$$

$$k_2^\mathrm{b} = \frac{1}{\sinh\lambda(L-l)}[k_3^\mathrm{b}\sigma_\mathrm{a}(\sinh\lambda L - \sinh\lambda l) + \sigma_\mathrm{d}\sinh\lambda L + k_4^\mathrm{b}\sigma^T(\sinh\lambda L - \sinh\lambda l)] \tag{A.23}$$

$$k_3^\mathrm{b} = \frac{F_3C_2 - C_3F_2}{C_1F_3 - C_3F_1 - \overline{F}} \tag{A.24}$$

$$k_4^\mathrm{b}\sigma^T = \frac{F_3C_4\sigma^T - C_3F_4\sigma^T}{C_1F_3 - C_3F_1 - \overline{F}} \tag{A.25}$$

References

Bennett, J.A., Young, R.J., 1998. The effect of fibre-matrix adhesion upon crack bridging in fibre reinforced composites. Composites Part A 29A, 1071–1081.

Bent, A.A., 1997. Active fibre composites for structural actuation. Thesis for PhD, Massachusetts Institute of Technology.

Buchanan, D.J., John, R., Johnson, D.A., 1997. Determination of crack bridging stresses from crack opening displacement profiles. International Journal of Fracture 87, 107–117.

Budiansky, B., Evans, A.G., Hutchinson, J.W., 1995. Fibre-matrix debonding effects on cracking in aligned fibre ceramic composites. International Journal of Solids and Structures 32 (3/4), 315–328.

Cox, B.N., 1993. Scaling for bridged cracks. Mechanics of Materials 15, 87–98.

Cox, B.N., Marshall, D.B., 1994. Concepts for bridged cracks in fracture and fatigue. Acta Metallurgica et Materialia 42 (2), 341–363.

Evans, A.G., Dalgleish, B.J., 1993. The fracture resistance of metal–ceramic interface. Materials Science and Engineering A 162, 1–13.

Kim, J.-K., Mai, Y.-W., 1991. High strength, high fracture toughness fibre composites with interface control—a review. Composites Science and Technology 41, 333–337.

Kim, J.-K., Mai, Y.-W., 1998. Engineering Interfaces in Fibre-Reinforced Composite. Elsevier, Oxford.

Larson, M.C., Miles, H., 1998. On the effects of friction, roughness and toughness on interfacial sliding in brittle composites. Mechanics of Materials 27, 77–89.

Liu, H.-Y., Mai, Y.-W., 2000. Evaluation of interface properties from a fibre fragmentation test. In: Proceedings of the Second Asian–Australasian Conference on Composites Materials. ACCM-2000, Korea.

Liu, H.-Y., Zhang, X., Mai, Y.-W., Diao, X.-X., 1999. On steady-state fibre pull-out, Part II: computer simulation. Composites Science and Technology 59, 2191–2199.

Pizzochero, A., 1998. Residual actuation and stiffness properties of piezoelectric composites: theory and experiment. Thesis for Master degree, Massachusetts Institute of Technology.

Qin, Q.-H., 2001. Fracture Mechanics of Piezoelectric Materials. WIT Press, Southampton, Boston.

Standard product catalog, Piezo System, Inc., 1999, 42, http://www.piezo.com.

Timoshenko, S.P., Goodier, J.N., 1970. Theory of Elasticity, third ed. McGraw-Hill, New York.

Xia, Z.C., Carr, R.R., Hutchinson, J.W., 1993. Transverse cracking in fibre-reinforced brittle matrix, cross-ply laminations. Acta Metallurgica et Materialia 41 (8), 2365–2376.

Xia, Z.C., Hutchinson, J.W., Evans, A.G., Budiansky, B., 1994. On large scale sliding in fibre-reinforced composites. Journal of Mechanics and Physics of Solids 42 (7), 1139–1158.

Zhang, X., Liu, H.-Y., Mai, Y.-W., Diao, X.-X., 1999. On steady-state fibre pull-out, Part I: the stress field. Composite Science and Technology 59, 2179–2189.

Zhang, X., Liu, H.-Y., Mai, Y.-W., 2002. A finite element study of the effects of interfacial debonding and sliding on fracture behaviour of fibre-reinforced composites. Composites Part A, submitted for publication.

Zok, F.W., Begley, M.R., Steyer, T.E., Walls, D.P., 1997. Inelastic deformation of fibre composites containing bridged cracks. Mechanics of Materials 26, 81–92.